

Sparsity-leveraging Reconfiguration of Smart Distribution Systems

Emiliano Dall'Anese and Georgios B. Giannakis

Abstract—A system reconfiguration problem is considered for three-phase smart power distribution networks featuring distributed generation, with the objective of finding the topology that minimizes the overall active power loss. In lieu of binary line selection variables, the notion of group sparsity is advocated to re-formulate the *nonconvex* distribution system reconfiguration (DSR) problem into a *convex* one. Using the duality theory, it is shown that the line selection task boils down to a shrinkage and thresholding operation on the line currents. Further, numerical tests illustrate the ability of the proposed scheme to identify the optimally meshed, weakly-meshed, or even radial configurations by adjusting a sparsity-tuning parameter in the DSR cost. Constraints on the voltages are investigated, and incorporated in the novel DSR problem to effect voltage regulation.

Index Terms—Smart distribution systems, microgrid, system reconfiguration, convex programming, compressive sampling.

I. INTRODUCTION

The fundamental objective of distribution system reconfiguration (DSR) schemes is to identify the topology of a distribution network that minimizes the overall active power loss [1], [2], [3]. DSR byproducts include balancing the network load [4], increasing the system security, and prompt (possibly network-wide) power delivery restoration in case of localized network failures. Computationally-affordable DSR schemes are increasingly advocated in modern distribution networks to enhance their efficiency and stability in the presence of distributed generation (DG), energy storage devices, as well as dispatchable and elastic loads [5].

Changes in the network topology are effected by opening or closing tie and sectionalizing line switches. These switching operations can be either performed manually in situ, or, commanded remotely by a network controller. Thus, the DSR task is traditionally approached by associating a binary selection variable with each switch [6], [7], [8], [9], [10], [11]. Unfortunately, this choice renders the resultant topology selection problem *NP-hard* [12], and thus challenging to solve optimally and efficiently. This explains why heuristic schemes have been largely employed to select the status of the switches. For example, all switches are initially assumed closed in e.g., [1], [8], and then they are progressively opened to eliminate (part of) the loops. A search over relevant radial configurations based

on approximate power flow methods is advocated in [2]. Alternative methods rely on fuzzy multi-objective [13], branch-and-bound [6], and genetic algorithms [9]. Off-the-shelf solvers for mixed-integer nonlinear programs were employed in e.g. [10] to solve a joint DSR and optimal power flow (OPF) for balanced systems, while Newton methods in conjunction with branch-selection heuristic techniques were employed in [7]. However, computational complexity of these schemes may become prohibitive as the size of the network increases, and no optimality guarantees are in general available for the obtained configuration.

The present paper leverages contemporary compressive sampling tools [14], [15] to bypass binary optimization variables, and formulate a novel *convex* DSR problem. Convexity here implies that interior point solvers can be utilized to solve the challenging DSR problem efficiently and optimally even for distribution networks of large size, and with densely deployed line switches. DSR solvers able to find a new configuration in a few seconds (or even less than one second, as shown for the IEEE 37-node feeder [16]) are instrumental for network operators to quickly re-shape the distribution grid in case of localized outages [17], and to gauge optimal topologies in case of abrupt load or generation variations.

The proposed convex formulation hinges on the notion of *group-sparsity*, an underlying attribute of the currents flowing on the phases of distribution lines equipped with switches. This group-sparse problem structure allows one to discard binary optimization variables, and select the states of the switches by augmenting the DSR cost with a convex sparsity-promoting regularization function [14], [15]. As in conventional (group) sparse linear regression, it is shown here that the line selection task boils down to a shrinkage and thresholding operation on the line currents. This is further corroborated through experiments on a modified version IEEE 37-node feeder [16], where a meshed, weakly-meshed, or radial configuration is obtained by simply adjusting a sparsity-tuning parameter. Differently from DSR approaches applicable to balanced distribution networks [2], [8], [10], [11], the problem formulated here accounts for unbalanced loads and non-zero off-diagonal entries of line admittance matrices.

Unfortunately, PQ loads and DG units (modeled as PQ loads as well) involve challenging nonlinear power flow relations. However, since the aim here is to develop a DSR scheme that is computationally efficient and yet able to reliably discard lines involving high active power losses, the powerful approximate load model developed in [18] is advocated, and tailored to the three-phase setup. Although this load model introduces an approximation error (which becomes negligible for sufficiently

This work was supported by the Inst. of Renewable Energy and the Environment (IREE) grant no. RL-0010-13, Univ. of Minnesota. Authors are with the Digital Technology Center and the Dept. of ECE, University of Minnesota, 200 Union Street SE, Minneapolis, MN 55455, USA. E-mails: {emiliano, georgios}@umn.edu

This work has been submitted for publication to the IEEE Transactions on Power Delivery on March 20, 2013.

large values the nominal voltage as shown analytically in [18], and further corroborated numerically here), the payoff here is huge, since a *convex* DSR problem can be formulated even in the presence of PQ loads.

II. PRELIMINARIES AND PROBLEM FORMULATION

Consider a portion of the power distribution grid located downstream of the distribution substation, that supplies a number of industrial and residential loads, and may include DG¹. The considered three-phase network is modeled also as a directed graph $(\mathcal{N}, \mathcal{E})$, where N nodes are collected in the set $\mathcal{N} := \{1, \dots, N\}$, and overhead or underground lines are represented by the set of (directed) edges $\mathcal{E} := \{(m, n)\} \subset \mathcal{N} \times \mathcal{N}$. Let node 1 represent the point of common coupling (PCC), taken to be the distribution substation. Distribution systems typically have tie and sectionalizing switches, whose states (closed or open) determine the topology of the network. Thus, let $\mathcal{E}_R \subset \mathcal{E}$ collect the branches equipped with controllable switches.

Let $\mathcal{P}_{mn} \subseteq \{a_{mn}, b_{mn}, c_{mn}\}$ and $\mathcal{P}_n \subseteq \{a_n, b_n, c_n\}$ denote the set of phases of line $(m, n) \in \mathcal{E}$ and node $n \in \mathcal{N}$, respectively; $I_{mn}^\phi \in \mathbb{C}$ the complex current flowing from node m to node n on phase ϕ ; $I_m^\phi \in \mathbb{C}$ the current injected at node $m \in \mathcal{N}$ and phase $\phi \in \mathcal{P}_m$; and, $V_m^\phi \in \mathbb{C}$ the complex line-to-ground voltage at the same node and phase. Lines $(m, n) \in \mathcal{E}$ are modeled as π -equivalent components [19, Ch. 6], and the $|\mathcal{P}_{mn}| \times |\mathcal{P}_{mn}|$ phase impedance matrix is denoted by $\mathbf{Z}_{mn} \in \mathbb{C}^{|\mathcal{P}_{mn}| \times |\mathcal{P}_{mn}|}$. Matrix \mathbf{Z}_{mn} is symmetric, full-rank, and it is obtained from the line primitive impedance matrix via Kron reduction [19, Ch. 4]. Using \mathbf{Z}_{mn} , the $|\mathcal{P}_{mn}| \times 1$ vector $\mathbf{i}_{mn} := [\{I_{mn}^\phi\}_{\phi \in \mathcal{P}_{mn}}]^\mathcal{T}$ collecting the currents flowing on each phase of line $(m, n) \in \mathcal{E}$ can be expressed as

$$\mathbf{i}_{mn} = \mathbf{Z}_{mn}^{-1}([\mathbf{v}_m]_{\mathcal{P}_{mn}} - [\mathbf{v}_n]_{\mathcal{P}_{mn}}) \quad (1)$$

with $\mathbf{v}_m := [\{V_m^\phi\}_{\phi \in \mathcal{P}_m}]^\mathcal{T}$. Let $\mathbf{i}_n := [\{I_n^\phi\}_{\phi \in \mathcal{P}_n}]^\mathcal{T}$ be the vector collecting the currents injected at node n , and $\{\mathbf{e}_n^\phi\}_{\phi \in \mathcal{P}_n}$ and $\{\mathbf{e}_{mn}^\phi\}_{\phi \in \mathcal{P}_{mn}}$ the canonical bases of $\mathbb{R}^{|\mathcal{P}_n|}$ and $\mathbb{R}^{|\mathcal{P}_{mn}|}$, respectively. Further, per-node $n \in \mathcal{N}$, define the $|\mathcal{P}_n| \times |\mathcal{P}_{mn}|$ matrix $\mathbf{A}_{jn}^{(n)} := \sum_{\phi \in \mathcal{P}_n} \mathbb{I}_{\{\phi \in \mathcal{P}_{mn}\}} \mathbf{e}_n^\phi (\mathbf{e}_{mn}^\phi)^\mathcal{T}$. Suppose for brevity, that the entries of the line shunt admittance matrix are negligible (they are, in fact, typically on the order of 10 – 100 micro Siemens per mile [16]). On the other hand, consider at the expense of minimally increasing complexity, that perceptible effects of shunt admittances can be readily accounted for in the ensuing problem formulations. Under these conditions, and using the definition of $\mathbf{A}_{jn}^{(n)}$,

¹Notation: Upper (lower) boldface letters will be used for matrices (column vectors); $(\cdot)^\mathcal{T}$ for transposition; $(\cdot)^*$ complex-conjugate; and, $(\cdot)^\mathcal{H}$ complex-conjugate transpose; $\Re\{\cdot\}$ denotes the real part, and $\Im\{\cdot\}$ the imaginary part; $j = \sqrt{-1}$ represents the imaginary unit; and $\mathbb{I}_{\{\cdot\}}$ is the indicator function ($\mathbb{I}_{\{x\}} = 1$ if x is true, and zero otherwise). $|\mathcal{P}|$ denotes the cardinality of set \mathcal{P} ; \mathbb{R}^N and \mathbb{C}^N represent the space of the $N \times 1$ real and complex vectors, respectively. Given a vector \mathbf{v} and a matrix \mathbf{V} , $[\mathbf{v}]_{\mathcal{P}}$ denotes a $|\mathcal{P}| \times 1$ sub-vector containing entries of \mathbf{v} indexed by the set \mathcal{P} , and $[\mathbf{V}]_{\mathcal{P}_1, \mathcal{P}_2}$ the $|\mathcal{P}_1| \times |\mathcal{P}_2|$ sub-matrix with row and column indexes described by \mathcal{P}_1 and \mathcal{P}_2 . Further, $\|\mathbf{v}\|_2 := \sqrt{\mathbf{v}^\mathcal{T} \mathbf{v}}$ denotes the ℓ_2 norm of \mathbf{v} . Finally, $\mathbf{0}_{M \times N}$ and $\mathbf{1}_{M \times N}$ denote $M \times N$ matrices with all zeroes and ones, respectively.

Kirchhoff's current law can be written per node n as

$$\mathbf{i}_n + \sum_{j \in \mathcal{N}_{\rightarrow n}} \mathbf{A}_{jn}^{(n)} \mathbf{i}_{jn} - \sum_{k \in \mathcal{N}_{n \rightarrow}} \mathbf{A}_{nk}^{(n)} \mathbf{i}_{nk} = \mathbf{0}_{|\mathcal{P}_n| \times 1} \quad (2)$$

where $\mathcal{N}_{\rightarrow n} := \{j : (j, n) \in \mathcal{E}\}$ and $\mathcal{N}_{n \rightarrow} := \{k : (n, k) \in \mathcal{E}\}$, respectively. Clearly, $\mathbf{i}_n = \mathbf{0}_{|\mathcal{P}_n| \times 1}$ if neither loads nor DG units are connected at node n .

Let $S_{mn} := \mathbf{i}_{mn}^\mathcal{H} [\mathbf{v}_m]_{\mathcal{P}_{mn}}$ denote the total complex power injected on line (m, n) from node m . If no power is dispelled through the distribution line $(m, n) \in \mathcal{E}$, S_{mn} coincides with the total power transferred to node n ; that is, $S_{mn} = -S_{nm}$. A necessary condition for this identity to hold is to have an identically zero line impedance matrix. In fact, it readily follows from (1) that $S_{mn} + S_{nm} = \mathbf{i}_{mn}^\mathcal{H} \mathbf{Z}_{mn} \mathbf{i}_{mn}$, and thus the total active power loss on line $(m, n) \in \mathcal{E}$ amounts to

$$\Delta P_{mn} := \Re\{S_{mn} + S_{nm}\} = \Re^\mathcal{T}\{\mathbf{i}_{mn}\} \Re\{\mathbf{Z}_{mn}\} \Re\{\mathbf{i}_{mn}\} + \Im^\mathcal{T}\{\mathbf{i}_{mn}\} \Re\{\mathbf{Z}_{mn}\} \Im\{\mathbf{i}_{mn}\}. \quad (3)$$

However, since typical values of \mathbf{Z}_{mn} in overhead and underground distribution segments render ΔP_{mn} not negligible [16], [19], it is desirable to select the topology (meaning the states of switches on lines \mathcal{E}_R), and adjust the complex line currents $\{\mathbf{i}_{mn}\}$ traversing the selected lines, so that the overall real power loss $\sum_{(m,n) \in \mathcal{E}} \Delta P_{mn}$ is minimized [1], [2].

Similar to various DSR renditions [6], [7], [8], [9], [10], [11], the topology selection problem will be first formulated in the ensuing subsection using binary line selection variables. However, since lines may be non-transposed and the spacings between conductors may be non-equilateral [19], the off-diagonal elements of \mathbf{Z}_{mn} are non-zero [16], [19]. Thus, different from DSR schemes tailored to balanced distribution networks (as in e.g., [2], [8], [10], [11]), the problem formulated here is able to capture current-coupling effects on the distribution lines.

A. Plain-vanilla DSR formulation

Suppose for the moment that loads are modeled using ideal current generators (that absorb current from the network). PQ loads and DG power injections (which follow a constant PQ model as well [20]) will be considered in Section II-B. Similar to [6], [7], [8], [9], [10], [11], associate a binary variable $x_{mn} \in \{0, 1\}$ with line $(m, n) \in \mathcal{E}_R$, and suppose that this distribution segment is used to deliver power to the loads if $x_{mn} = 1$. In this case, the DSR problem can be formulated as follows [cf. (2)]

$$(P1) \min_{\{\mathbf{i}_{mn}\}, \{x_{mn}\}} \sum_{(m,n) \in \mathcal{E}} \Re^\mathcal{T}\{\mathbf{i}_{mn}\} \Re\{\mathbf{Z}_{mn}\} \Re\{\mathbf{i}_{mn}\} + \Im^\mathcal{T}\{\mathbf{i}_{mn}\} \Re\{\mathbf{Z}_{mn}\} \Im\{\mathbf{i}_{mn}\} \quad (4a)$$

subject to (2), and

$$\Re^2\{[\mathbf{i}_{mn}]_\phi\} + \Im^2\{[\mathbf{i}_{mn}]_\phi\} \leq I_{mn}^{\max}, \quad (m, n) \in \mathcal{E} \setminus \mathcal{E}_R \quad (4b)$$

$$\Re^2\{[\mathbf{i}_{mn}]_\phi\} + \Im^2\{[\mathbf{i}_{mn}]_\phi\} \leq I_{mn}^{\max} x_{mn}, \quad (m, n) \in \mathcal{E}_R \quad (4c)$$

$$x_{mn} \in \{0, 1\}, \quad (m, n) \in \mathcal{E}_R \quad (4d)$$

where constraints (4b)–(4c) are enforced on each phase $\phi \in \mathcal{P}_{mn}$, and $I_{mn}^{\max} \geq 0$ is a cap for $|I_{mn}^\phi|^2$. Clearly, when

$x_{mn} = 0$, \mathbf{i}_{mn} is forced to zero by (4c), thus implying that line $(m, n) \in \mathcal{E}_R$ is not used (see also [6], [7], [10], [11]). When the desired topology is radial, additional constraints are present [10], [11]. In particular, suppose that the graph $(\mathcal{N}, \mathcal{E})$ contains N_I cycles, and collect in the set \mathcal{C}_i the lines forming cycle $i = 1, \dots, N_I$. Then, to obtain a tree network, it suffices to add in (P1) the constraint $\sum_{(m,n) \in \mathcal{C}_i} x_{mn} \leq |\mathcal{C}_i| - 1$ per cycle i .

Matrices $\{\Re\{\mathbf{Z}_{mn}\} \in \mathbb{R}^{|\mathcal{P}_{mn}| \times |\mathcal{P}_{mn}|}\}$ are typically positive definite and full-rank (see e.g., the real test cases in [16]); thus, it follows that the DSR cost (4a) is strictly convex. However, presence of the binary variables $\{x_{mn}\}$ renders (P1) a mixed-integer quadratic program (MIQP), which is *nonconvex* and *NP-hard* [12]. Finding its global optimum requires solving a number of subproblems (one per switch status) that increases exponentially ($2^{|\mathcal{E}_R|}$) in the number of switches. This explains why heuristic schemes have been largely employed to select the network topology [2], [6], [8], [13]. Alternatively, off-the-shelf solvers for mixed-integer (non)linear programs [10] and genetic algorithms [9] have been employed. However, since these solvers are in general computationally-heavy, they are not suited for optimizing the operation of medium- and large-size distribution networks, or, for finding a post-outage system configuration in order to efficiently restore power delivery network-wide [17].

In the ensuing Section III, compressive sampling tools will be advocated to bypass binary selection variables, and reformulate the DSR problem into a *convex* one. But first, an approximate yet powerful load model is outlined next.

B. Approximate load model

Consider the well-established “exponential model” relating injected (or supplied) powers with voltages $\{V_n^\phi\}$ and currents $\{I_n^\phi\}$ (see e.g., [20])

$$V_n^\phi (I_n^\phi)^* = S_n^\phi \left| \frac{\sqrt{3}}{V_N} V_n^\phi \right|^{\kappa_n}, \quad \phi \in \mathcal{P}_n, n \in \mathcal{N} \setminus \{1\} \quad (5)$$

where V_N is the nominal line-line voltage magnitude of the system (e.g., 4.8 kV for the IEEE 37-node feeder [16]); S_n^ϕ is the net complex power that would be injected on phase ϕ of node n if V_n^ϕ were equal to the nominal voltage $\frac{\sqrt{3}}{V_N} e^{j\varphi_N^\phi}$, $\varphi_N^\phi \in \{0^\circ, -120^\circ, 120^\circ\}$; and, $\kappa_n \in \{0, 1, 2\}$ is a model parameter. Specifically, constant PQ, constant current, and constant impedance loads are obtained by setting $\kappa_n = 0$, $\kappa_n = 1$, and $\kappa_n = 2$, respectively.

DG units are typically modeled as constant PQ loads (that supply power); thus, let $\mathcal{S} \subset \mathcal{N}$ be the (sub)set of nodes where DG units are present, and $\mathbf{s}_{G,n} := [\{S_{G,n}^\phi\}]^T$ the vector collecting the complex power $S_{G,n}^\phi$ supplied by these units on each phase of node n . Notice that multiple DG units may be present at each node; if this is the case, $S_{G,n}^\phi$ can be readily replaced by $\sum_{u=1}^{N_U} S_{G,n,u}^\phi$, with N_U the number of DG units at node n . Per phase $\phi \in \mathcal{P}_n$, let $S_{L,n}^\phi$ denote the complex power demanded by a wye-connected load at the bus n . Finally, define $\mathbf{s}_{L,n} := [\{S_{L,n}^\phi\}]^T$, and suppose as usual that the voltages

at the substation $\mathbf{v}_1 := [\frac{\sqrt{3}}{V_N} e^{j0^\circ}, \frac{\sqrt{3}}{V_N} e^{j-120^\circ}, \frac{\sqrt{3}}{V_N} e^{j120^\circ}]^T$ are taken as reference for the phasorial representation [19].

As elaborated further in Section IV, the use of the nonlinear relation (5) in (P1) introduces an additional source of non-convexity [10], and would render the DSR formulated in the next section nonconvex. This, in turn, would exacerbate the problem complexity, and would make optimality claims on the obtained topology difficult to establish. Instead, the aim here is to develop a DSR scheme that is computationally efficient yet able to reliably (and optimally) discard lines involving high active power losses. Developing such a scheme is instrumental for network operators to quickly re-shape the distribution grid in case of e.g. abrupt load or generation variations, and to promptly restore the power delivery network-wide after an outage event [17].

To this end, the powerful approximate load model derived in [18] is advocated to relate injected currents to complex powers linearly. Specifically, upon defining the vectors $\boldsymbol{\iota}_n := [\Re\{\mathbf{i}_n\}, \Im\{\mathbf{i}_n\}]^T$ and $\boldsymbol{\sigma}_{G,n} := [\Re\{\mathbf{s}_{G,n}\}, \Im\{\mathbf{s}_{G,n}\}]^T$, it follows from [18] that the current injected at node n can be approximated as

$$\boldsymbol{\iota}_n \approx \underbrace{\frac{\sqrt{3}}{V_N} \begin{bmatrix} \Re\{\boldsymbol{\Phi}_n\} & \Im\{\boldsymbol{\Phi}_n\} \\ \Im\{\boldsymbol{\Phi}_n\} & -\Re\{\boldsymbol{\Phi}_n\} \end{bmatrix}}_{:=\mathbf{g}_n(\boldsymbol{\sigma}_{G,n})} (\boldsymbol{\sigma}_{G,n} - \boldsymbol{\sigma}_{L,n}) \quad (6)$$

with $\boldsymbol{\Phi}_n := \text{diag}(\{e^{j\varphi_N^\phi}\}_{\phi \in \mathcal{P}_n})$, and $\boldsymbol{\sigma}_{G,n} = \mathbf{0}$ for $n \in \mathcal{N} \setminus (\{1\} \cup \mathcal{S})$. The approximation error incurred by (6) is infinitesimal for large nominal voltages V_N as analytically shown in [18], and further corroborated by the tests on the IEEE 37-node feeder reported in the Appendix. Specifically, the average error is just on the order of 0.1 Ampere (a relative error of less than 2% - which yields an error on the powers that is on the order of the load prediction error). The motivation behind (6) is twofold: first, using (6) in conjunction with compressive sampling methods, offers the advantage of a convex DSR problem for a system featuring PQ loads. Further, from an DSR standpoint, this approximation does not jeopardize the ability of the methods proposed in the ensuing sections to efficiently capture the topology yielding the lowest power loss. Based on this topology, voltages and currents are as usual fine-tuned in a subsequent optimization stage by employing more sophisticated techniques such as OPF.

III. DSR VIA GROUP-SPARSITY

Collect first the real and imaginary parts of \mathbf{i}_{mn} in the vector $\boldsymbol{\xi}_{mn} := [\Re\{\mathbf{i}_{mn}\}, \Im\{\mathbf{i}_{mn}\}]^T \in \mathbb{R}^{2|\mathcal{P}_{mn}|}$, and define matrices $\mathbf{Z}_{mn} := \mathbf{I}_2 \otimes \Re\{\mathbf{Z}_{mn}\}$, $\mathbf{A}_{mn}^{(m)} := \mathbf{I}_2 \otimes \mathbf{A}_{mn}^{(m)}$, and $\mathbf{M}_{mn}^\phi := \mathbf{I}_2 \otimes \mathbf{e}_{mn}^\phi (\mathbf{e}_{mn}^\phi)^T$, where \mathbf{I}_2 is the 2×2 identity matrix. Key to obtaining a convex re-formulation of (P1) is to notice that the entries of $\boldsymbol{\xi}_{mn}$ are *all* zero if line $(m, n) \in \mathcal{E}_R$ is not used to deliver power to the loads. In compressive sampling, this translates to having the vectors $\{\boldsymbol{\xi}_{mn} | (m, n) \in \mathcal{E}_R\}$ being *group-sparse* [14]; meaning that, either $\boldsymbol{\xi}_{mn} = \mathbf{0}$, or, the elements of $\boldsymbol{\xi}_{mn}$ may all be nonzero. One powerful way to capitalize on this attribute of currents flowing on lines equipped with switches, consists in augmenting the cost (4a)

with the following sparsity-promoting regularization term [14]

$$r(\{\xi_{mn}\}) := \sum_{(m,n) \in \mathcal{E}_R} \lambda \|\xi_{mn}\|_2 \quad (7)$$

where λ is a real positive constant. Then, using (7), and discarding binary line selection variables, the DSR problem can be re-formulated as:

$$(P2) \quad \min_{\{\xi_{mn}\}, \{\sigma_{G,n}\}} \frac{1}{2} \sum_{(n,m) \in \mathcal{E}} \xi_{mn}^T \bar{Z}_{mn} \xi_{mn} + r(\{\xi_{mn}\}) \quad (8a)$$

$$\text{subject to} \quad \sigma_{G,n}^{\min} \leq \sigma_{G,n} \leq \sigma_{G,n}^{\max}, \forall n \in \mathcal{S} \quad (8b)$$

$$\mathbf{g}_n(\sigma_{G,n}) + \sum_{j \in \mathcal{N}_{\rightarrow n}} \bar{A}_{jn}^{(n)} \xi_{jn} = \sum_{k \in \mathcal{N}_{\rightarrow n}} \bar{A}_{nk}^{(n)} \xi_{nk} \quad (8c)$$

$$\xi_{mn}^T \bar{M}_{mn}^\phi \xi_{mn} \leq I_{mn}^{\max}, \forall \phi, (m,n) \in \mathcal{E} \quad (8d)$$

where Kirchhoff's current law (8c) is enforced at each node $n \in \mathcal{N}$, and (8b) are box constraints for the power supplied by controllable DG units. Matrices $\{\bar{Z}_{mn}\}$ are positive definite, while matrices $\{\bar{M}_{mn}^\phi\}$ are symmetric, positive semidefinite, with rank 2. Thus, (P2) is convex, and it can be solved optimally via general-purpose interior point methods. What is more, (P2) can be reformulated as a second-order cone program (SOCP), and thus solved using efficient primal-dual interior point methods tailored to SOCP (see e.g., [21]).

The role of λ in $r(\{\xi_{mn}\})$ is to control the number of vectors $\{\xi_{mn}\}_{(m,n) \in \mathcal{E}_R}$ (and, hence, of currents $\{\mathbf{i}_{mn}\}_{(m,n) \in \mathcal{E}_R}$) that are set to zero. When $\lambda = 0$, all branches \mathcal{E}_R are traversed by a non-zero current. Then, with λ increasing, the number of lines where no current is flowing increases [14]. This implies that by adjusting λ one can obtain either meshed topologies (low values of λ), weakly-meshed, or even radial systems (high values of λ). To rigorously show this, results from duality theory [22] are leveraged next to derive closed form expressions for the optimal line currents.

Let $\{\mu_n\}$ and $\{\rho_{mn}^\phi\}$ denote the multipliers associated with (8c) and (8d), respectively, and consider the (partial) Lagrangian function of (P2), namely:

$$\begin{aligned} \mathcal{L}(\xi, \sigma_G, \mu, \rho) := & \frac{1}{2} \sum_{(n,m) \in \mathcal{E}} \xi_{mn}^T \bar{Z}_{mn} \xi_{mn} + r(\{\xi_{mn}\}) \\ & + \sum_{n=1}^N \mu_n^T \left(\mathbf{g}_n(\sigma_{G,n}) + \sum_{j \in \mathcal{N}_{\rightarrow n}} \bar{A}_{jn}^{(n)} \xi_{jn} - \sum_{k \in \mathcal{N}_{\rightarrow n}} \bar{A}_{nk}^{(n)} \xi_{nk} \right) \\ & + \sum_{(n,m) \in \mathcal{E}} \sum_{\phi \in \mathcal{P}_{mn}} \rho_{mn}^\phi \left(\xi_{mn}^T \bar{M}_{mn}^\phi \xi_{mn} - I_{mn}^{\max} \right) \end{aligned} \quad (9)$$

where $\xi := \{\xi_{mn}\}$, $\sigma_G := \{\sigma_{G,n}\}$, and likewise μ, ρ collect all the dual variables for brevity. Given (9), the dual function and the dual problem take the form

$$\mathcal{D}(\mu, \rho) := \min_{\xi, \sigma_{G,n}^{\min} \leq \sigma_{G,n} \leq \sigma_{G,n}^{\max}} \mathcal{L}(\xi, \sigma_G, \mu, \rho) \quad (10)$$

$$\mathcal{D}^{\text{opt}} = \max_{\{\mu_n \geq 0\}, \rho} \mathcal{D}(\mu, \rho). \quad (11)$$

Since (P2) is convex, if there exists a feasible solution ξ, σ_G such that $\xi_{mn}^T \bar{M}_{mn}^\phi \xi_{mn} < I_{mn}^{\max}$ for all $(m,n) \in \mathcal{E}$ and $\sigma_{G,n}^{\min} < \sigma_{G,n} < \sigma_{G,n}^{\max}$ for all $n \in \mathcal{S}$ (that is, Slater's condition

holds), then (P2) has zero duality gap [22, Ch. 6]. Suppose that this is the case, and let $\xi^{\text{opt}}, \sigma_G^{\text{opt}}$ and $\mu^{\text{opt}}, \rho^{\text{opt}}$ denote the optimal primal and dual solutions, respectively. The Lagrangian optimality condition [22, Prop. 6.2.5] asserts that ξ^{opt} and σ_G^{opt} are also the minimizers of (10) for $\mu = \mu^{\text{opt}}$ and $\rho = \rho^{\text{opt}}$; that is $\mathcal{D}^{\text{opt}}(\mu^{\text{opt}}, \rho^{\text{opt}}) = \mathcal{L}(\xi^{\text{opt}}, \sigma_G^{\text{opt}}, \mu^{\text{opt}}, \rho^{\text{opt}})$. Thus, re-arranging terms of the Lagrangian function in a convenient way, and exploiting the decomposability of (9), it turns out that the optimal currents flowing on the phases of line (m,n) are given as the solution of the sub-problem:

$$\xi_{mn}^{\text{opt}} = \arg \min_{\xi_{mn}} \frac{1}{2} \xi_{mn}^T \bar{Z}_{mn} \xi_{mn} + \lambda \|\xi_{mn}\|_2 - \mu_{mn}^T \xi_{mn} \quad (12)$$

where $\lambda = 0$ for lines $(m,n) \in \mathcal{E} \setminus \mathcal{E}_R$ (whereas $\lambda > 0$ for all lines \mathcal{E}_R), and

$$\tilde{Z}_{mn} := \bar{Z}_{mn} + \sum_{\phi \in \mathcal{P}_{mn}} \rho_{mn}^{\phi, \text{opt}} \bar{M}_{mn}^\phi \quad (13)$$

$$\mu_{mn} := \bar{A}_{mn}^{(m)T} \mu_m^{\text{opt}} - \bar{A}_{mn}^{(n)T} \mu_n^{\text{opt}}. \quad (14)$$

Since \tilde{Z}_{mn} is positive definite and $\sum_{\phi} \rho_{mn}^{\phi, \text{opt}} \bar{M}_{mn}^\phi$ positive semidefinite, it follows that \tilde{Z}_{mn} is positive definite and invertible. Thus, based on (12), the optimal line currents are obtained next.

Proposition 1: Per line $(m,n) \in \mathcal{E} \setminus \mathcal{E}_R$, the optimal currents ξ_{mn}^{opt} are given by

$$\xi_{mn}^{\text{opt}} = \tilde{Z}_{mn}^{-1} \mu_{mn}. \quad (15)$$

Proposition 2: If $(m,n) \in \mathcal{E}_R$ is a single-phase distribution line, then the optimal current $\xi_{mn}^{\phi, \text{opt}} = [\Re\{I_{mn}^\phi\}, \Im\{I_{mn}^\phi\}]^T$ on phase ϕ is given by the following soft-thresholding vector operation

$$\xi_{mn}^{\phi, \text{opt}} = \frac{[\|\mu_{mn}\|_2 - \lambda]_+}{(\Re\{Z_{mn}^\phi\} + \rho_{mn}^{\phi, \text{opt}}) \|\mu_{mn}\|_2} \mu_{mn} \quad (16)$$

where $[a]_+ := \max\{0, a\}$. For lines $(m,n) \in \mathcal{E}_R$ that are two- or three-phase, the optimal vector of line currents ξ_{mn}^{opt} is obtained via the following shrinkage and thresholding vector operation

$$\xi_{mn}^{\text{opt}} = \eta^{\text{opt}} \mathbb{I}_{\{\|\mu_{mn}\|_2 > \lambda\}} \left(\eta^{\text{opt}} \tilde{Z}_{mn} + \frac{\lambda^2}{2} \mathbf{I}_{2|\mathcal{P}_{mn}|} \right)^{-1} \mu_{mn} \quad (17)$$

where $\eta^{\text{opt}} \in \mathbb{R}^+$ is the solution of the scalar optimization problem

$$\min_{\eta \geq 0} \eta - \frac{\eta}{2} \mu_{mn}^T \left(\eta \tilde{Z}_{mn} + \frac{\lambda^2}{2} \mathbf{I}_{2|\mathcal{P}_{mn}|} \right)^{-1} \mu_{mn}. \quad (18)$$

Proof. Consider first the case of single-phase distribution lines, where (12) boils down to

$$\begin{aligned} \xi_{mn}^{\text{opt}} = \arg \min_{\xi_{mn}} & \frac{1}{2} (\Re\{Z_{mn}^\phi\} + \rho_{mn}^{\phi, \text{opt}}) \xi_{mn}^T \xi_{mn} \\ & - \mu_{mn}^T \xi_{mn} + \lambda \|\xi_{mn}\|_2. \end{aligned} \quad (19)$$

The solver of (19) takes the form $\xi_{mn} = z \mu_{mn}$ for some scalar $z \geq 0$. In fact, among all possible ξ_{mn} with the

same ℓ_2 -norm, the Cauchy-Schwarz inequality implies that the maximizer of $\mu_{mn}^\top \xi_{mn}$ is colinear with (and in the same direction of) μ_{mn} . Thus, substituting $\xi_{mn} = z\mu_{mn}$ into (19) yields the following problem in the scalar z :

$$z^{opt} = \arg \min_{z \geq 0} \frac{1}{2} (\Re\{Z_{mn}^\phi\} + \rho_{mn}^{\phi, opt}) z^2 \|\mu_{mn}\|_2 - z \|\mu_{mn}\|_2 + \lambda |z| \quad (20)$$

where $\lambda|z|$ can be replaced by λz since $z \geq 0$. The necessary and sufficient condition for z to minimize (23) is [23, p. 92]

$$\begin{cases} \|\mu_{mn}\|_2 \leq \lambda, & \text{if } z^{opt} = 0 \\ \Re\{Z_{mn}^\phi\} + \rho_{mn}^{\phi, opt} - \|\mu_{mn}\|_2 + \lambda = 0, & \text{if } z^{opt} \neq 0 \end{cases} \quad (21)$$

which is satisfied by

$$z^{opt} = \frac{1}{(\Re\{Z_{mn}^\phi\} + \rho_{mn}^{\phi, opt}) \|\mu_{mn}\|_2} [\|\mu_{mn}\|_2 - \lambda]_+. \quad (22)$$

Relations (17)–(18) can be proved along the lines of [15]. Specifically, (12) is first equivalently reformulated as the following quadratic program with a second-order conic constraint

$$\begin{aligned} \min_{\xi_{mn}, t} \quad & \frac{1}{2} \xi_{mn}^\top \tilde{Z}_{mn} \xi_{mn} + \lambda \|\xi_{mn}\|_2 - \mu_{mn}^\top \xi_{mn} + t \\ \text{subject to} \quad & \begin{bmatrix} -\lambda \xi_{mn} \\ -t \end{bmatrix} \preceq 0 \end{aligned} \quad (23)$$

Next, derive the (concave) dual problem of (23), which amounts to

$$\begin{aligned} \max_{\chi} \quad & -\frac{1}{2} (\mu_{mn} + \lambda \chi)^\top \tilde{Z}_{mn}^{-1} (\mu_{mn} + \lambda \chi) \\ \text{subject to} \quad & \|\chi\|_2^2 \leq 1 \end{aligned} \quad (24)$$

where the constraint $\chi \in \text{range}(\tilde{Z}_{mn})$ is left implicit, and χ is the multiplier associated with the conic constraint in (23). Consider then the Lagrange dual of (24), namely

$$\min_{\eta \geq 0} \max_{\chi} -\frac{1}{2} (\mu_{mn} + \lambda \chi)^\top \tilde{Z}_{mn}^{-1} (\mu_{mn} + \lambda \chi) - \eta \|\chi\|_2^2 + \eta. \quad (25)$$

Recalling that \tilde{Z}_{mn} is invertible, it turns out that the optimal solution of (25) is given by

$$\chi = -\frac{\lambda}{2} \left(\eta \tilde{Z}_{mn} + \frac{\lambda^2}{2} \mathbf{I} \right)^{-1} \mu_{mn} \quad (26)$$

with η as in (18). Notice that the eigenvalues of $(\eta^{opt} \tilde{Z}_{mn} + \frac{\lambda^2}{2} \mathbf{I})^{-1}$, denoted by $\{\theta_i\}$ for brevity, satisfy the inequality $0 < \theta_i \leq 2/\lambda^2$ for all $i = 1, \dots, 2|\mathcal{P}_{mn}|$. Thus, when $\|\mu_{mn}\|_2 \leq \lambda$, the term $(1/2) \mu_{mn}^\top \left(\eta \tilde{Z}_{mn} + \frac{\lambda^2}{2} \mathbf{I}_{2|\mathcal{P}_{mn}|} \right)^{-1} \mu_{mn}$ in (18) is negative, thus implying that $\eta^{opt} = 0$. \square

Some comments are now due in order to interpret the role of the multipliers $\{\mu_n^{opt}\}$ and $\{\rho_{mn}^{\phi, opt}\}$ in view of Ohm's Law, and to better appreciate the merits of the sparsity-promoting regularization term $r(\{\xi_{mn}\})$. Notice first that from the complementary slackness condition [22, Prop. 6.2.5], one has that $\rho_{mn}^{\phi, opt} = 0$ whenever the corresponding constraint (8d) is not active. Suppose temporarily that $\rho_{mn}^{\phi, opt} = 0$ for all lines, in which case \tilde{Z}_{mn} boils down to $\tilde{Z}_{mn} = \mathbf{I}_2 \otimes \Re\{Z_{mn}\}$ [cf. (9)].

Since currents and voltages abide by Ohm's Law, (15)–(16) imply that the legitimate unit for $\{\mu_{mn}\}$ is the volt. In particular, comparing (15) with (1) reveals that μ_{mn}^{opt} corresponds to the electrical potential difference between two nodes m and n connected by a line with a resistive matrix $\Re\{Z_{mn}\}$; that is, $\mu_{mn}^{opt} = [\Re\{Z_{mn}\} \mathbf{i}_{mn}]$, $\Im\{Z_{mn}\} \mathbf{i}_{mn}]^\top$. In other words, μ_{mn} represents the contribution to the potential difference $\mathbf{v}_m - \mathbf{v}_n$ that is due to the resistive part of Z_{mn} .

With this connotation of μ_{mn} , it follows from (16) that single-phase lines equipped with a switch can be characterized by a “virtual” line resistance, whose values is given by $\Re\{Z_{mn}^\phi\}$ amplified by a factor $\|\mu_{mn}\|_2 / [\|\mu_{mn}\|_2 - \lambda]_+$. This resistive boost discourages high currents on line (m, n) , something that in compressive sampling is usually referred to as “shrinkage operation” [14], [15]. Eventually, when $\|\mu_{mn}\|_2 < \lambda$, the value of this virtual resistance goes to infinity, thus resembling an open switch. Notice further that the thresholding operator $[\|\mu_{mn}\|_2 - \lambda]_+$ naturally suggests the order of magnitude of the parameter λ that has to be used to (de)select a line. Although less intuitive, this shrinkage and thresholding operation effected through $\lambda \|\xi_{mn}\|_2$ can be noticed also in (17) for lines with two and three phases. Here, the design variable η is expressed in watt. Finally, variable $\rho_{mn}^{\phi, opt}$ can be interpreted as an additional “virtual” resistance added to the conductor ϕ of line (m, n) when the currents reaches its maximum allowable value I_{mn}^{\max} . In principle, since this extra resistive value introduce an additional virtual active power loss, higher values of I_{mn}^{ϕ} are discouraged.

The optimal topology of the network is obtained by discarding the distribution lines with an associated zero current. That is, $\mathcal{E}^{opt} := \mathcal{E} \setminus \{(m, n) \in \mathcal{E}_R : \xi_{mn}^{opt} = \mathbf{0}\}$. Further, the optimal line currents are readily computed as $\mathbf{i}_{mn}^{opt} := [\xi_{mn}^{opt}]_{1:|\mathcal{P}_{mn}|} + j[\xi_{mn}^{opt}]_{|\mathcal{P}_{mn}|+1:2|\mathcal{P}_{mn}|}$. Thus, given the voltage vector \mathbf{v}_1 at the substation, and the optimal set of distribution lines \mathcal{E}^{opt} , voltages $\{\mathbf{v}_n\}_{n=2}^N$ can be readily obtained by using (1) iteratively. Although (P2) is grounded on the affine approximation (6), it will be shown in Section V that the deviation between the load profile and the output of the DSR problem is on average less than 2 kW for the IEEE 37-node feeder [16] - something on the order of the load forecasting error. Further, tests on this system revealed that it is possible to solve (P2) in less than 1 second (as opposed to several seconds or minutes required by solvers of mixed-integer nonlinear programs and genetic algorithms), thus rendering the proposed method particularly suitable for e.g., fast post-outage power delivery restoration purposes [17].

Finally, notice that in order to encourage the use of specific lines $(m, n) \in \mathcal{E}_R$, the regularization function (7) can be replaced by its weighted counterpart $r'(\{\xi_{mn}\}) := \sum_{(m, n) \in \mathcal{E}_R} \lambda_{mn} \|\xi_{mn}\|_2$, with $\lambda_{mn} \geq 0$ for all (m, n) . For example, if the use of a line (j, k) is inadvisable due to e.g., ongoing maintenance or security concerns, a higher associated weight $\lambda_{jk} > \lambda_{mn}$ should be selected.

IV. ACCOUNTING FOR VOLTAGE CONSTRAINTS

Similar to various DSR renditions, the objective of (P2) is to obtain a topology that is likely to yield the lowest power

losses for a given predicted load profile. Based on the resultant optimal configuration $(\mathcal{N}, \mathcal{E}^{opt})$, voltages and currents are fine-tuned in a subsequent optimization stage where more sophisticated techniques such as OPF are employed (see e.g., [24] and references therein). In some cases however, it may be desirable to introduce voltage regulation-related constraints in order to avoid network configurations that can potentially yield infeasible OPF solutions (meaning a set of voltages returned by the OPF solver not within prescribed minimum and maximum utilization limits).

To effect voltage regulation, consider introducing a constraint $V_n^\phi \in \mathcal{B}_n^\phi$ per node $n \in \mathcal{N} \setminus \{1\}$ and phase $\phi \in \mathcal{P}_n$, where \mathcal{B}_n^ϕ is a given closed set collecting the admissible voltages (see e.g., [10], [19]); set \mathcal{B}_n^ϕ will be exemplified in the ensuing Sections IV-A and IV-B. One way to enforce these constraints is to let the voltages become optimization variables, and formulate a joint DSR and OPF problem as in, e.g. [10]. However, it is not convenient here to have voltages as optimization variables because:

- i) equality (5) is nonconvex (as in OPF problems); and,
- ii) when binary variables are used to model the states of switches [6], [7], [8], [9], [10], [11], and constraints (4c) are employed [6], [10], [11], the solver would set $\mathbf{i}_{mn}^{opt} = \mathbf{0}$ for lines with $x_{mn} = 0$. However, it is clear from (1) that imposing $\mathbf{i}_{mn}^{opt} = \mathbf{0}$ requires equating voltages at the two end points of line (m, n) ; that is, $[\mathbf{v}_m]_{\mathcal{P}_{mn}} = [\mathbf{v}_n]_{\mathcal{P}_{mn}}$. This artifact renders the joint DSR and OPF problem infeasible in various practical cases. Consider for example a network with 5 nodes, lines $\mathcal{E} = \{(1, 2), (2, 3), (2, 4), (2, 5), (3, 5), (4, 5)\}$, and switches in $\mathcal{E}_R = \{(2, 3), (2, 4), (2, 5)\}$. Suppose that only one switch must be closed in order to obtain a radial network, and this switch is the one on line $(2, 3)$. However, by setting $\mathbf{v}_2 = \mathbf{v}_4 = \mathbf{v}_5$, the load demands at nodes 4 and 5 would not be satisfied, since no power is delivered at these nodes.

One approach to resolving this issue is to discard (4c) and replace $\{\mathbf{Z}_{mn}\}_{(m,n) \in \mathcal{E}_R}$ with $\{\mathbf{Z}_{mn}x_{mn}\}_{(m,n) \in \mathcal{E}_R}$. However, the resultant formulation yields a challenging bilinear problem with integer variables. Aiming at a computationally affordable DSR scheme, voltages are treated here as *latent* problem variables as shown next.

Recall from Section II-B that voltages at the substation $\boldsymbol{\nu}_1 := [\Re\{\mathbf{v}_1\}, \Im\{\mathbf{v}_1\}]^T$ are typically taken as a reference for the phasorial representation [19]. Consider the network in Fig. 1. Given $\boldsymbol{\nu}_1$, and assuming that the arc $(1, 2)$ originates at node 1 and ends at 2, voltages at node 2 can be expressed as [cf. (1)]

$$\boldsymbol{\nu}_2 = \boldsymbol{\nu}_1 - \underbrace{\begin{bmatrix} \Re\{\mathbf{Z}_{12}\} & -\Im\{\mathbf{Z}_{12}\} \\ \Im\{\mathbf{Z}_{12}\} & \Re\{\mathbf{Z}_{12}\} \end{bmatrix}}_{:= \boldsymbol{\Psi}_{12}} \boldsymbol{\xi}_{12}. \quad (27)$$

Likewise, if the sequence of nodes $\mathcal{W}_{1 \rightarrow n} := \{1, \dots, n\}$ forms an undirected path $1 \rightarrow 2 \rightarrow \dots \rightarrow n$ from the substation to node n , and *none* of the lines $(m, n) : m, n \in \mathcal{W}_{1 \rightarrow n}$ is equipped with switches, then $\boldsymbol{\nu}_n$ can be expressed as $\boldsymbol{\nu}_n = \boldsymbol{\nu}_1 + \sum_{(m,n): m,n \in \mathcal{W}_{1 \rightarrow n}} \alpha_{mn} \boldsymbol{\Psi}_{mn} \boldsymbol{\xi}_{mn}$, where $\alpha_{mn} = 1$ if the path traverses the directed edge (m, n) (which goes from m to n) in the opposite direction, and $\alpha_{mn} = -1$ otherwise. A

similar approach was taken in [6]. Based on these relations, voltage regulation can be readily effected by adding to (P2) the following constraint per node n :

$$\boldsymbol{\nu}_1 + \sum_{(m,n): m,n \in \mathcal{W}_{1 \rightarrow n}} \alpha_{mn} \boldsymbol{\Psi}_{mn} \boldsymbol{\xi}_{mn} \in \mathcal{B}_n. \quad (28)$$

Once (P2) is solved, voltages are computed based on \mathcal{E}^{opt} as shown in Section III. When switches are densely deployed, there may not exist an undirected path connecting the substation to a node n that includes only lines in $\mathcal{E} \setminus \mathcal{E}_R$. If this is the case, the substation must be replaced by another point of reference; that is, a node where the value (or an approximate value) of the voltages can be unequivocally determined. From the model set forth in Section II-B (see also [18]), it can be noticed that approximate values of the voltages are readily available for nodes with a nonzero load demand; in fact, given the approximate injected currents $\boldsymbol{\nu}_n$ in (6), a reference voltage can be obtained via (5). Hereafter, the reference node will be generically denoted by n_{ref} . Two possible choices for the set \mathcal{B}_n are presented in the ensuing subsections.

A. Box constraints

Let $\hat{V}_{n,\Re}^\phi$ and $\check{V}_{n,\Re}^\phi$ be upper and lower bounds, respectively, on the real part of voltage V_n^ϕ . Likewise, let $\hat{V}_{n,\Im}^\phi$ and $\check{V}_{n,\Im}^\phi$ denote the counterparts for $\Im\{V_n^\phi\}$. Then, upon collecting these quantities for all phases $\phi \in \mathcal{P}_n$ in the vectors $\hat{\boldsymbol{\nu}}_n := [\{\hat{V}_{n,\Re}^\phi\}, \{\hat{V}_{n,\Im}^\phi\}]^T$ and $\check{\boldsymbol{\nu}}_n := [\{\check{V}_{n,\Re}^\phi\}, \{\check{V}_{n,\Im}^\phi\}]^T$, (P2) can be readily reformulated as follows:

$$\begin{aligned} (P2') \quad & \min_{\{\boldsymbol{\xi}_{mn}\}, \{\boldsymbol{\sigma}_{G,n}\}} \frac{1}{2} \sum_{(n,m) \in \mathcal{E}} \boldsymbol{\xi}_{mn}^T \bar{\mathbf{Z}}_{mn} \boldsymbol{\xi}_{mn} + r(\{\boldsymbol{\xi}_{mn}\}) \\ & \text{subject to } (8b), (8c), (8d), \text{ and} \\ & \check{\boldsymbol{\nu}}_n \preceq \boldsymbol{\nu}_{n_{ref}} + \sum_{(m,n): m,n \in \mathcal{W}_{n_{ref} \rightarrow n}} \alpha_{mn} \boldsymbol{\Psi}_{mn} \boldsymbol{\xi}_{mn} \preceq \hat{\boldsymbol{\nu}}_n. \end{aligned} \quad (29)$$

Problem (P2') is convex, and thus efficiently (and optimally) solved via either general-purpose interior point methods, or, primal-dual schemes tailored to SOCP [21]. Through (29) it is possible to constrain both the magnitude of V_n^ϕ and its deviation from the nominal phase $\angle V_{n_{ref}}^\phi$. Further, introducing these additional constraints does not alter the expressions for the optimal line currents provided in Propositions 1 and 2.

B. Nonconvex constraints on voltage magnitudes

In traditional OPF approaches, it is usual to consider lower and upper bounds on the voltage magnitudes, which habitually coincide with minimum and maximum utilization and service voltage levels [19]. Consider then introducing in (P2) the constraints $\hat{V}_n \leq |V_n^\phi| \leq \check{V}_n$, per node n and phase $\phi \in \mathcal{P}_n$.

This leads to the following DSR reformulation:

$$(P2'') \min_{\{\xi_{mn}\}, \{\sigma_{G,n}\}} \frac{1}{2} \sum_{(n,m) \in \mathcal{E}} \xi_{mn}^T \bar{Z}_{mn} \xi_{mn} + r(\{\xi_{mn}\})$$

subject to (8b), (8c), (8d), and

$$\hat{V}_n^2 \leq \left(\nu_{nref} + \sum_{m,n} \alpha_{mn} \Psi_{mn} \xi_{mn} \right)^T Q_n^\phi$$

$$\times \left(\nu_{nref} + \sum_{m,n} \alpha_{mn} \Psi_{mn} \xi_{mn} \right) \leq \check{V}_n^2, \phi \in \mathcal{P}_n \quad (30)$$

where $Q_n^\phi := \mathbf{I}_2 \otimes \text{diag}(\mathbf{e}_n^\phi)$. Unfortunately, the constraint $-(\nu_{nref} + \Psi \xi)^T Q_n^\phi (\nu_{nref} + \Psi \xi) + \hat{V}_n^2 \leq 0$, where Ψ and ξ are defined in the obvious way, is nonconvex since the function on the left hand side is concave. However, this source of non-convexity can be efficiently addressed by resorting to convex approximation techniques. Among candidate methods, the successive convex approximation (SCA) approach proposed in [25] is well suited for the problem at hand because it guarantees first-order Karush–Kuhn–Tucker (KKT) optimality under mild regularity conditions.

To briefly illustrate the general SCA method, consider an optimization problem

$$\min_{\xi \in \mathcal{I}} f_0(\xi) \quad (31a)$$

$$\text{subject to } f_k(\xi) \leq 0, \quad k = 1, 2, \dots, K \quad (31b)$$

where $f_0(\xi)$ is convex and differentiable, $f_k(\xi)$, $k = 1, \dots, K$, are differentiable functions, and the feasible region $\mathcal{F} := \{\xi \in \mathcal{I} | f_k(\xi) \leq 0, k = 1, \dots, K\}$ is compact. Then, starting from a feasible point $\xi^{(0)} \in \mathcal{F}$, a series of approximate problems can be solved to locate a KKT optimal point of the original (non-convex) problem. For each $k = 1, \dots, K$, let $\tilde{f}_k(\xi; \xi^{(j)})$ denote the surrogate function for $f_k(\xi)$, which may depend on the solution $\xi^{(j)}$ to the problem in the $(j-1)$ -st iteration. The approximate problem to solve in iteration j is

$$\min_{\xi \in \mathcal{I}} f_0(\xi) \quad (32a)$$

$$\text{subject to } \tilde{f}_k(\xi; \xi^{(j)}) \leq 0, \quad k = 1, 2, \dots, K \quad (32b)$$

whose feasible region is denoted as $\mathcal{F}^{(j)}$. Provided that $\tilde{f}_k(\xi; \xi^{(j)})$ satisfies the following conditions c1)–c3) for each $k = 1, \dots, K$, the series of solutions $\xi^{(j)}$, $j = 1, 2, \dots$, to the approximate problems converges to the KKT point of the original problem (31):

- c1) $f_k(\xi) \leq \tilde{f}_k(\xi; \xi^{(j)}), \quad \forall \xi \in \mathcal{F}^{(j)}$
- c2) $f_k(\xi^{(j)}) = \tilde{f}_k(\xi^{(j)}; \xi^{(j)})$
- c3) $\nabla f_k(\xi^{(j)}) = \nabla \tilde{f}_k(\xi^{(j)}; \xi^{(j)})$.

In order to apply the SCA method to $(P2'')$, an appropriate surrogate constraint for the nonconvex lower bound in (30) needs to be determined. Since, $-(\nu_{nref} + \Psi \xi)^T Q_n^\phi (\nu_{nref} + \Psi \xi)$ is quadratic and concave, a linear approximation around the feasible point $\{\xi_{mn}^{(j)}\}$ satisfying c1)–c3) can be readily found. In fact, after standard manipulations, it follows that the convex problem to

be solved at iteration j of the SCA algorithm is:

$$(P2''^{(j)}) \min_{\{\xi_{mn}\}, \{\sigma_{G,n}\}} \frac{1}{2} \sum_{(n,m) \in \mathcal{E}} \xi_{mn}^T \bar{Z}_{mn} \xi_{mn} + r(\{\xi_{mn}\})$$

subject to (8b), (8c), (8d), and

$$(\mathbf{a}_n^\phi(\xi^{(j)}))^T (\xi^{(j)} - \xi) - b_n^\phi(\xi^{(j)}) + \hat{V}_n^2 \leq 0 \quad (33a)$$

$$(\nu_{nref} + \Psi \xi)^T Q_n^\phi (\nu_{nref} + \Psi \xi) \leq \check{V}_n^2 \quad (33b)$$

with

$$\mathbf{a}_n^\phi(\xi^{(j)}) := 2\Psi^T Q_n^\phi (\nu_{nref} + \Psi \xi^{(j)}) \quad (33c)$$

$$b_n^\phi(\xi^{(j)}) := (\nu_{nref} + \Psi \xi^{(j)})^T Q_n^\phi (\nu_{nref} + \Psi \xi^{(j)}) \quad (33d)$$

The resultant SCA algorithm amounts to solving a sequence of convex problems $(P2''^{(0)}) \rightarrow \dots \rightarrow (P2''^{(j)}) \rightarrow \dots$, where the feasible point $\xi^{(j)}$ is taken to be the solution of $(P2''^{(j-1)})$ (and $\xi^{(0)}$ is an arbitrary initial feasible point). Convergence of this scheme is formalized next (see also [25]).

Proposition 3: Given an initial feasible point $\xi^{(0)}$, the iterates $\xi^{(j)}$ generated by $(P2''^{(j)})$, $j = 0, 1, 2, \dots$, converge to a KKT solution of the nonconvex DSR problem $(P2'')$.

In the ensuing section, the proposed DSR algorithms are tested on the IEEE 37-node feeder [16].

V. NUMERICAL EXPERIMENTS

Consider the IEEE 37-node feeder [16], which is a portion of the three-phase 4.8 kV distribution network located in California. Compared to the scheme in [16], 8 additional three-phase lines equipped with sectionalizing switches are considered, as shown in Fig 1. The parameters of these additional lines are listed in Table I, where the admittance matrices corresponding to the configuration indexes 723 and 724 can be found in [16]. The line impedance matrices for the original lines are computed as specified in [16]. A balanced load of 85 kW and 40 kVAr per phase is added to node 23 to represent an additional residential demand. Further, DG units are located at nodes 9, 13, 15, 19, 26, 32, and 36. These units operate at unity power factor, and can supply a maximum power of 50 kW per phase. Two different setups are considered, depending on the number and locations of switches:

- 1) Test 1: $\mathcal{E}_{R,1} = \{(8, 14), (6, 20), (10, 16), (20, 26), (16, 24), (10, 17), (24, 33), (26, 35)\}$; and,
- 2) Test 2: $\mathcal{E}_{R,2} = \mathcal{E}_{R,1} \cup \{(17, 22), (23, 24), (23, 25), (29, 30)\}$.

The voltage at the distribution substation is set to $\mathbf{v}_1 = [1\angle 0^\circ, 1\angle -120^\circ, 1\angle 120^\circ]^T$ pu. Finally, box constraints on the voltages are considered; specifically, the lower and upper bounds of the real and imaginary parts of the voltages are such that $\Re\{V_m^\phi\} \in [\Re\{V_1^\phi\} - 0.0354, \Re\{V_1^\phi\} + 0.0354]$ pu and $\Im\{V_m^\phi\} \in [\Im\{V_1^\phi\} - 0.0354, \Im\{V_1^\phi\} + 0.0354]$ pu. This translates to having the magnitude of the voltages in the range $|V_n^\phi| \in [0.95, 1.05]$ pu.

The optimization package CVX², along with the interior-point based solver SeDuMi³ are employed to solve the DSR

²[Online] Available: <http://cvxr.com/cvx/>

³[Online] Available: <http://sedumi.ie.lehigh.edu/>

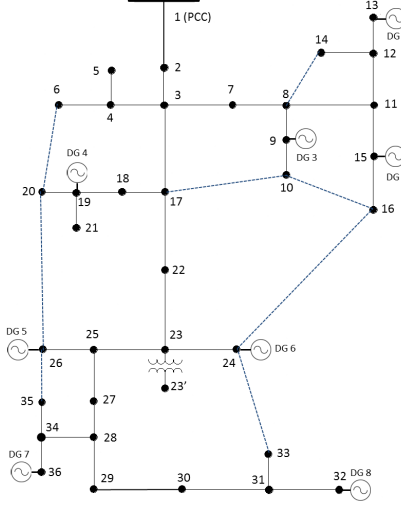


Fig. 1. Modified IEEE 37-bus test feeder.

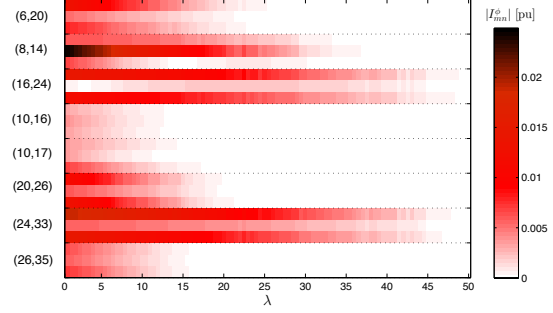
problems in MATLAB. The average computational time required by SeDuMi to solve the DSR problem was 0.4 seconds on a machine with Intel Core i7-2600 CPU @ 3.40GHz.

TABLE I
ADDITIONAL LINES IN THE MODIFIED IEEE 37-NODE FEEDER

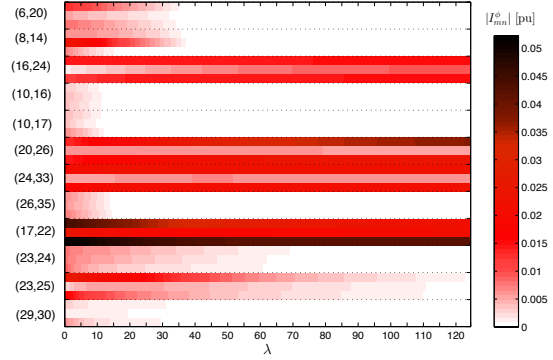
Line	Conf.	Length (ft)	Line	Conf.	Length (ft)
(8,14)	723	1144	(16,24)	724	1580
(6,20)	724	1320	(10,17)	724	1137
(10,16)	724	847	(24,33)	724	1315
(20,26)	724	815	(26,35)	724	377

Fig. 2 depicts the magnitude of currents flowing on lines equipped with switches, for different values of the sparsity-promoting parameter λ . Three rows per line are reported, where the first row corresponds to phase “a,” and the third one to phase “c” (all lines are three-phase). The voltage magnitude is color-coded, where white represents a zero current (that is, an open switch), while red hues are used to capture different values for $|I_n^\phi| > 0$, in pu. In the upper plot (a), it can be clearly seen that the number of open switches increases as λ increases, and the original tree topology described in [16] is obtained at saturation. Interestingly, the first lines that are discarded are (10,16) and (10,17), which implies that the majority of the power supplied to that part of the network comes from the DG units. As expected, similar trends are evidenced in Fig. 2(b) for Test 2, thus further corroborating the merits of the proposed method based on sparsity-promoting regularizations. It can be noticed that at saturation only four switches are left closed and, interestingly, the resultant tree topology is different than the original one in [16]. In fact, the switches in (23,24), (23,25) are open, while lines (16,24), (20,26), and (24,33) are used to deliver power to the loads.

Fig. 3 reports the expected active power loss as a function of λ , for both cases. Notice first that power losses are in general lower in Test 2. Then, it can be clearly seen that the power loss monotonically increases as λ increases (that is, with the number of open switches). This motivates augmenting the cost of (P_2) with a term that accounts for the possible maintenance



(a) Test 1.



(b) Test 2.

Fig. 2. Absolute value of the currents on lines \mathcal{E}_R , for different λ .

costs of lines and switches, in order to find a possible trade-off between active power loss and number of utilized lines. If this economical cost incurred by the use of a line is modeled by using a strictly convex function, the optimal λ can be efficiently found via bisection.

Since the linear relation (6) introduces an approximation error when PQ loads are present, the average deviation from the nominal loads is quantified next. Specifically, the deviation for the real power is defined as $\Delta P = (1/\sum_n |\mathcal{P}_n^L|) \sum_n \sum_\phi |P_n^\phi - \hat{P}_n^\phi|$, where \mathcal{P}_n^L is a set collecting the phases at node n with a non-zero load; $\hat{P}_{L,m}^\phi$ is the output of the DSR scheme; and $P_n^\phi = P_{G,n}^\phi - P_{L,n}^\phi$ is the true real power that would be obtained by considering the exact nonlinear relation (5). The counterpart ΔQ is defined in a similar way. These deviations yield only $\Delta P = 1.49$ kW and $\Delta Q = 0.92$ kVar for Test 1, and $\Delta P = 1.35$ kW and $\Delta Q = 0.85$ kVar for Test 2. The error is very small, and does not jeopardize optimality of the obtained topology (as would happen in case of higher approximation errors).

The magnitude of the voltages V_n^ϕ are reported in Fig. 4 for different values of λ . The substation voltages are not included. Voltages are computed as explained in Section III, once the optimal topology has been identified. As expected, the “cloud” formed by all the voltage magnitudes $\{|V_n^\phi|\}$ is confined within the considered lower and upper bounds, which are marked with red dotted lines. Fig. 5 reports the active power supplied by the DG units. It can be seen that in both cases the majority of DG units supplies 50 kW, which

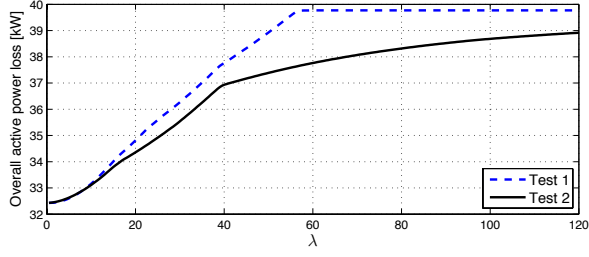
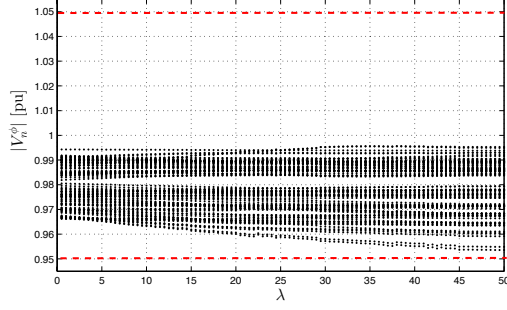
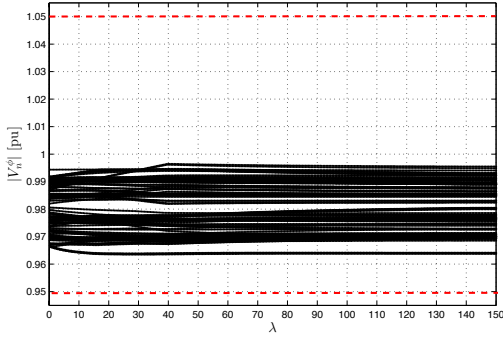


Fig. 3. Overall active power loss [kW].



(a)



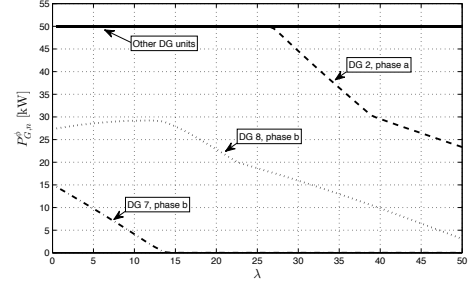
(b)

Fig. 4. Voltage magnitude at the nodes [pu]. (a) Test 1. (b) Test 2.

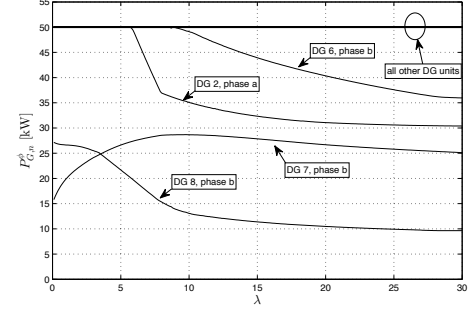
corresponds to the maximum power that can be generated. In Fig. 5(a) the power supplied by DG units 7 and 8 is smaller, or even zero, on phase “b.” This is because the load of that part of the network on phase “b” is relatively low, and using those DG units to supply loads that are electrically far from nodes 32 and 36 incurs higher power losses on the lines. Similar conclusions can be drawn for Fig. 5(b). However, in this case, because of the new topology, DG units 7 and 8 are judiciously utilized to supply other loads.

VI. CONCLUDING REMARKS

A DSR problem was considered for three-phase distribution systems featuring DG. Leveraging the notion of group-sparsity, and adopting an approximate linear relation between powers and injected currents, a novel convex DSR formulation was proposed. Being convex, the proposed DSR problem can be solved efficiently even for distribution networks of large size. The ability of the proposed scheme to select the topologies



(a)



(b)

Fig. 5. Active power supplied by the DG units [kW]. (a) Test 1. (b) Test 2.

that minimize the overall active power loss was demonstrated via numerical tests, and it was also justified analytically.

APPENDIX

Fig. 6 reports magnitude (in pu) and phase of the injected (absorbed) currents for the IEEE 37-node feeder. The original scheme described in [16] is considered, with voltages and currents obtained by using the OPF solver proposed in [24]. Black, green, and orange circles correspond to the exact values of the currents for phases a, b, and c, respectively. These values of current magnitudes and phases are compared with the ones obtained by using the approximate relation (6), which are marked with “×”. It can be seen that the incurred approximation error is very small (see also the results reported in [18]). More precisely, the average error $\Delta := (1/\sum_n |\mathcal{P}_n^L|) \sum_n \sum_\phi |I_n^\phi - \hat{I}_n^\phi|$, where $\hat{I}_{L,m}^\phi$ is the current computed using (6) amounts to 0.1767 Ampere.

This approximation error is certainly acceptable for two reasons: first, using (6) in conjunction with compressive sampling methods, gives rise to the formulation of a convex DSR problem for a system featuring PQ loads. Secondly, voltages and currents are usually adjusted in a subsequent optimization stage via OPF.

REFERENCES

- [1] A. Merlin and H. Back, “Search for a minimal-loss operating spanning tree configuration in an urban power distribution system,” in *5th Power Syst. Computation Conf.*, Cambridge, U.K., Jul. 1975.
- [2] M. E. Baran and F. F. Wu, “Network reconfiguration in distribution systems for loss reduction and load balancing,” *IEEE Trans. Power Del.*, vol. 4, no. 2, pp. 1401–1407, Apr. 1989.

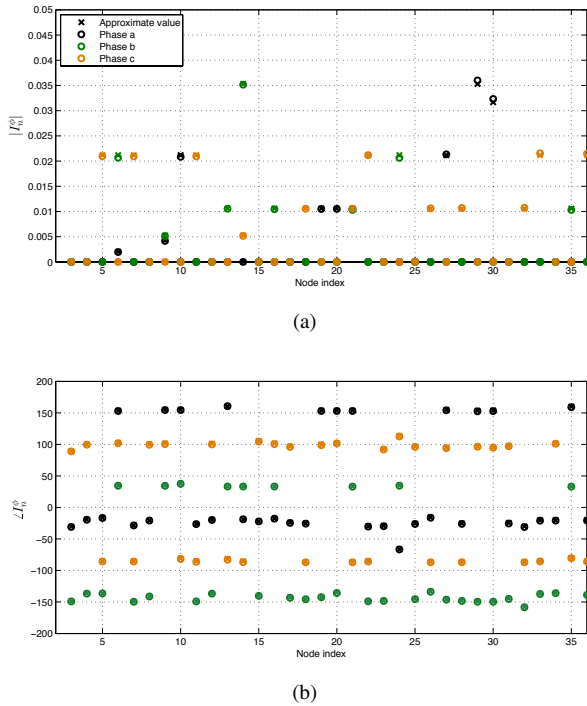


Fig. 6. True and approximate node currents. (a) Magnitudes. (b) Phases.

[3] D. Shirmohammadi and H. W. Hong, "Reconfiguration for electric distribution networks for resistive line loss reduction," *IEEE Trans. Power Del.*, vol. 4, no. 2, pp. 1492–1498, Apr. 1989.

[4] K. Y. Huang and H. C. Chin, "Distribution feeder energy conservation by using heuristics fuzzy approach," *Int. J. Elect. Power Energy Syst.*, vol. 24, no. 6, pp. 439–445, Aug. 2002.

[5] N. Hatziaegyriou, H. Asano, R. Iravani, and C. Marnay, "Microgrids: An overview of ongoing research, development, and demonstration projects," *IEEE Power & Energy Mag.*, vol. 5, no. 4, pp. 78–94, July–Aug. 2007.

[6] C. S. Chen and M. Y. Cho, "Energy loss reduction by critical switches," *IEEE Trans. Power Del.*, vol. 8, no. 3, pp. 1246–1253, Jul. 1993.

[7] H. P. Schmidt, N. Ida, N. Kagan, and J. C. Guaraldo, "Fast reconfiguration of distribution systems considering loss minimization," *IEEE Trans. Power Syst.*, vol. 20, no. 3, pp. 1311–1319, Aug. 2005.

[8] F. V. Gomes, S. Carneiro, J. Pereira, M. Vinagre, P. Garcia, and L. R. de Araujo, "A new distribution system reconfiguration approach using optimum power flow and sensitivity analysis for loss reduction," *IEEE Trans. Power Syst.*, vol. 21, no. 4, pp. 1616–1623, Nov. 2006.

[9] Y. C. Huang, "Enhanced genetic algorithm-based fuzzy multi-objective approach to distribution network reconfiguration," in *Proc. Inst. Elect. Eng., Gen. Transm. Distrib.*, vol. 149, no. 5, San Francisco, CA, Sep. 2002, pp. 615–620.

[10] H. M. Khodr, J. Martinez-Crespo, M. A. Matos, and J. Pereira, "Distribution systems reconfiguration based on OPF using Benders decomposition," *IEEE Trans. Power Del.*, vol. 24, no. 4, pp. 2166–2176, Oct. 2009.

[11] B. Moradzadeh and K. Tomovic, "Mixed integer programming-based reconfiguration of a distribution system with battery storage," in *44th North American Power Symposium*, University of Illinois at Urbana-Champaign, IL, Sep. 2012.

[12] G. L. Nemhauser and L. A. Wolsey, *Integer and Combinatorial Optimization*. Wiley, 1988.

[13] D. Das, "Reconfiguration of distribution system using fuzzy multi-objective approach," *Int. J. Elect. Power Energy Syst.*, vol. 28, no. 5, pp. 331–338, Jun. 2006.

[14] M. Yuan and Y. Lin, "Model selection and estimation in regression with grouped variables," *J. of the Royal Stat. Soc.*, vol. 68, pp. 49–67, 2006.

[15] A. T. Puig, A. Wiesel, G. Fleury, and A. O. Hero, "Multidimensional shrinkage-thresholding operator and group LASSO penalties," *IEEE Sig. Proc. Letters*, vol. 18, no. 6, pp. 363–366, Jun. 2011.

[16] W. H. Kersting, "Radial distribution test feeders," in *IEEE Power Engineering Society Winter Meeting*, vol. 2, 2001, pp. 908–912.

[17] G. Celli and F. Pilo, "Optimal sectionalizing switches allocation in distribution networks," *IEEE Trans. Power Del.*, vol. 14, no. 3, pp. 1167–1172, Jul. 1999.

[18] S. Bolognani and S. Zampieri, "A distributed control strategy for reactive power compensation in smart microgrids," *IEEE Trans. on Autom. Control*, 2013, to appear; see also <http://arxiv.org/pdf/1106.5626>.

[19] W. H. Kersting, *Distribution System Modeling and Analysis*. 2nd ed., Boca Raton, FL: CRC Press, 2007.

[20] IEEE Task Force on Load representation for dynamic performance, "Load representation for dynamic performance analysis," *IEEE Trans. Power Syst.*, vol. 8, no. 2, pp. 472–482, May 1993.

[21] M. Lobo, L. Vandenbergh, S. Boyd, and H. Lebert, "Applications of second-order cone programming," *Linear Algebra and its Applications*, no. 248, pp. 193–228, Nov. 1998.

[22] D. P. Bertsekas, A. Nedić, and A. Ozdaglar, *Convex Analysis and Optimization*. Athena Scientific, 2003.

[23] A. Ruszczyński, *Nonlinear Optimization*. Princeton Univ. Press, Princeton, NJ, 2006.

[24] E. Dall'Anese, H. Zhu, and G. B. Giannakis, "Distributed optimal power flow for smart microgrids," *IEEE Trans. Smart Grid*, 2013, to appear; see, also <http://arxiv.org/abs/1211.5856>.

[25] B. R. Marks and G. P. Wright, "A general inner approximation algorithm for nonconvex mathematical programs," *Oper. Res.*, vol. 26, no. 4, pp. 681–683, Jul.-Aug. 1978.